

Viscoelasticity of an Entangled Polymer Solution with Special Attention on a Characteristic Time for Nonlinear Behavior

Tadashi Inoue, Yasuhiro Yamashita, and Kunihiro Osaki*

Institute for Chemical Research, Kyoto University, Uji, Kyoto 611-0011, Japan

Received July 12, 2001; Revised Manuscript Received November 28, 2001

ABSTRACT: Nonlinear viscoelasticity was studied for a polystyrene solution in tricresyl phosphate; molecular weight = 5480 kg mol⁻¹; concentration = 49 kg m⁻³. The longest Rouse relaxation time, τ_R , was estimated by fitting the Rouse theory to dynamic modulus at high frequencies. The Doi–Edwards tube model theory presumes that $2\tau_R$ is the characteristic time for equilibration of chain contour length; $(2\tau_R)^{-1}$ is the rate for an extended chain to shrink back to equilibrium. The τ_R value was much lower than that evaluated with more widely accepted methods. However, the shear stress (σ) and the first normal stress difference (N_1) in the start-up of shear flow with low rate of shear ($<(2\tau_R)^{-1}/5$) were consistent with the assumption that the contour length is always at equilibrium value. At high rate of shear ($>8(2\tau_R)^{-1}$), the maxima of σ and N_1 were located at $t = 2\tau_R$ and $4\tau_R$, respectively, in accord with the interpretation that $2\tau_R$ is the characteristic time for chain shrink. The strain-dependent relaxation modulus, $G(t, \gamma)$, was also studied. At high magnitudes of shear, $\gamma = 4$ or 5, the ratio $G(t, \gamma)/G(t, 0)$ decreased rapidly around $t = 2\tau_R$ and leveled off at $t = 20(2\tau_R)$: the chain shrink process plays the main role in damping but a slower process may also be involved. At $\gamma = 1$ or less, $G(t, \gamma)/G(t, 0)$ decreased only at times much longer than $2\tau_R$. The damping of relaxation modulus involves some secondary process with a characteristic time longer than that of the chain contraction process.

Introduction

According to the tube model theory of entangled polymer, the origin of nonlinearity in viscoelasticity is the large difference between the orientational relaxation time of the whole chain and the equilibration time of chain contour length measured along the entanglement points.^{1–3a} The former corresponds to the longest stress relaxation time, τ_1 , and the latter to twice the longest Rouse relaxation time, $2\tau_R$, which is much shorter than τ_1 for well-entangled systems. The extended contour length in a large deformation returns to its equilibrium value with a characteristic time $2\tau_R$ when the flow is stopped, or the material shape is fixed, and so the stress at $t > 2\tau_R$ would be lower than expected from the linear viscoelasticity relation. The contour length is always at equilibrium in a continuous flow if the strain rate is sufficiently lower than $(2\tau_R)^{-1}$, and again the stress would be lower than the linear value.

Behavior of the strain-dependent relaxation modulus, $G(t, \gamma)$, for a polymer with sharp molecular weight distribution may represent the contour length equilibration process in material of fixed shape. It can be factorable as

$$G(t, \gamma) = G(t)h(\gamma) \quad (t > t_k) \quad (1)$$

at times longer than a certain critical time, t_k , which is approximately independent of γ .^{1–5} The damping function, $h(\gamma)$, representing how the stress is lower than the linear viscoelasticity limit, is in good agreement with the theoretical value. The critical time, t_k , was proportional to the square of the molecular weight for a few entangled polymer solutions.^{6,7} It was claimed that t_k was approximately equal to $5(2\tau_R)$, which seemed to be an appropriate time for an elongated chain to completely return to its equilibrium length, i.e., an explicit representation of the condition $t \gg 2\tau_R$. Theories seem to be in accord with this result.^{8–10} However, it was claimed

in a recent study that the previous evaluation of τ_R was erroneous and $t_k/2\tau_R$ might be much larger, approximately equal to 15, for a polystyrene solution.¹¹ Details of the new evaluation method of τ_R were given elsewhere.¹² Similar result for t_k value was reported by Archer et al. but its relation with τ_R value was not described so definitely; actually, three different methods for determining τ_R are cited in the paper.¹³ The implication of the critical time, t_k , seems unclear now, and this is partly due to the uncertainty in definition of τ_R .

The role of the chain contraction process has not been so quantitatively investigated in the case of continuous flow.³ Viscosity, η , and the coefficient of first normal stress difference, Ψ_1 , in steady shear flow decrease rather smoothly with rate of shear, $\dot{\gamma}$, and do not exhibit any particular features, such as sudden change of variation rate or leveling off, at the characteristic rate for chain contraction, $\dot{\gamma} = (2\tau_R)^{-1}$. According to one version (based on independent alignment assumption) of the original tube model theory, the stress is described with a K-BKZ constitutive equation.^{1–3,14,15} Then the shear stress and the first normal stress difference in shear flow can be completely derived from the data of $G(t, \gamma)$. The model predicts that at start-up of shear flow the magnitude of shear corresponding to the maximum of η is independent of $\dot{\gamma}$ and that Ψ_1 does not exhibit overshoot. These predictions and the calculated steady values of η and Ψ_1 are in good agreement with experimental results at low $\dot{\gamma}$. Discrepancies appear at a certain $\dot{\gamma}$ which may be related to the characteristic rate, $(2\tau_R)^{-1}$. This possibility has been occasionally mentioned but not examined quantitatively.

At high $\dot{\gamma}$, Ψ_1 as well as η exhibits overshoot. The maximum of each quantity does not correspond to a constant magnitude of shear, independent of $\dot{\gamma}$, but to a constant time of flow at very high $\dot{\gamma}$. A pioneering study¹⁶ reported that the maximum of η was located at about $t = \tau_R/4$ and that of Ψ_1 at $t = \tau_R/2$. A recent study

pointed out that the τ_R values in this study could be too large.¹² It was then proposed that τ_R should be determined from the dynamic modulus, $G'(\omega)$, in the frequency range where it is proportional to $\omega^{1/2}$. This frequency dependence is in accord with the Rouse theory¹⁷ so that a τ_R can be obtained by fitting the data to the theoretical curve. Careful determination of τ_R on this line gave a result that the times at the maxima of shear and normal stresses, t_{om} and t_{Nm} , at high rates of shear were approximately related to τ_R as follows:¹⁸

$$t_{om} = 2\tau_R \quad (2)$$

$$t_{Nm} = 4\tau_R \quad (3)$$

The observation of eqs 2 and 3 are in accord with modified versions of the tube model, in which the chain contour is allowed to be longer than the equilibrium length so that phenomena at high rates of shear can be treated.^{9,10} However, the result has not been unanimously accepted because the τ_R value used was much lower than those evaluated with other (more widely used) methods as discussed later.

On briefly reviewing the observations possibly related to chain contraction, we note that various methods of study, as referred to in the last three paragraphs, have been mostly performed separately, for different systems and different temperatures. Due to the differences in the evaluation methods of characteristic time, τ_R , detailed comparisons of different set of experiments are often difficult. Here we present a set of viscoelastic data for one typical sample at one temperature and examine nonlinear viscoelasticity in view of the characteristic time, τ_R . One purpose of the paper, in addition to the study of material behavior, is to provoke discussion toward obtaining an appropriate value of τ_R for describing nonlinear behavior. We employ one τ_R , evaluated from the complex modulus at high frequency, throughout this paper and compare various nonlinear viscoelasticity functions. The data of complex modulus are fully given as a fitting function so that other researchers could criticize the method in a quantitative way.

Method

Material. We chose a semidilute polystyrene solution in tricresyl phosphate, for which shear flow was stable over a wide range of rate of shear and the stepwise strain could be applied without wall slip. Polystyrene was a standard polymer, f550, with sharp molecular weight distribution from Toso Co., Ltd. Molecular weight was 5480 kg mol⁻¹ and concentration was 49 kg m⁻³ at 273 K.

Measurements. A standard rheometer (ARES; Rheometrics Scientific Far East) was used for all the measurements. The complex modulus was measured over a temperature range from 238 to 323 K and reduced to a reference temperature $T_r = 273$ K with the method of reduced variables.¹⁹ A vertical shift factor²⁰ approximately proportional to the absolute temperature was required to obtain good master curves as reported before.¹²

Strain-dependent relaxation modulus, $G(t, \gamma)$, was measured for $\gamma = 0.3, 0.7, 1, 2, 3, 4$, and 5 at 298 K. The strain was applied in less than 30 ms but the response of the stress transducer was not fast enough to get data at times less than 100 ms. The results were reduced to 273 K with the method of reduced variables. The shift factors were adapted from those for the complex modulus.

The shear stress and the first normal stress difference at the start-up of shear flow were measured at 283, 298, and 313 K and were reduced to the reference temperature, 273 K. The range of rate of shear was taken as wide as possible: The

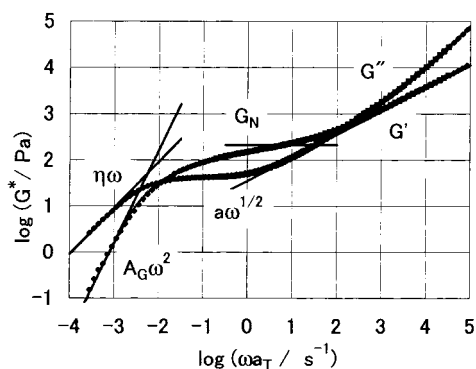


Figure 1. Real part, G' , and imaginary part, G'' , of the complex modulus at 273 K. Four straight lines indicate the definitions of various parameters.

lowest rate was determined by the detectable stress level and the highest by the stability of steady flow.

Results

Complex Modulus and Various Parameters. Figure 1 shows the master curves for the storage modulus, $G'(\omega)$, and the loss modulus, $G''(\omega)$. Data were taken at every 5 or 10 deg in the range 238–323 K and reduced to $T_r = 273$ K: $G'(\omega)/b_T$ and $G''(\omega)/b_T$ were plotted against ωa_T . The shift factors were represented by the following equations:

$$\log a_T = \frac{-4.7(T - T_r)}{86 + T - T_r} \quad (4)$$

$$b_T = \frac{T}{T_r} \quad (T \geq 263 \text{ K}) \quad (5)$$

The vertical shift factor, b_T , at lower temperatures is not proportional to T . The reduced data can be reproduced with the following fitting function

$$G'(\omega) + iG''(\omega) = \sum_{p=1}^N \frac{g_p i\omega\tau_p}{1 + i\omega\tau_p} + \frac{cRT_r^{N_R}}{M} \sum_{p=1}^{N_R} \frac{i\omega\tau_{Rp}}{1 + i\omega\tau_{Rp}} + i\omega\eta_\infty \quad (6)$$

where

$$g_p = \frac{9.5 \text{ Pa}}{0.995^{p-1}}, \quad \tau_p = \frac{310 \text{ s}}{1.5^{p-1}}, \quad N = 13$$

$$\tau_{Rp} = \frac{2.4 \text{ s}}{p^2}, \quad N_R = 1000, \quad \eta_\infty = 0.75 \text{ Pa s} \quad (7)$$

Any linear viscoelasticity functions for this material at $T \geq 263$ K can be produced with use of eqs 4 through 7. The set of equations and parameters are meant to be a compact form of a large data table and physical meaning is not sought. The functional form of the second term on rhs of eq 6 together with the form $\tau_{Rp} \propto p^{-2}$ was chosen for the convenience of determining τ_R from $G'(\omega)$ at high frequencies.¹²

The terminal flow and the rubbery plateau zones are mostly represented by the first term on the rhs of eq 6 and the low-frequency end of the glass-to-rubbery transition zone by the second term. τ_{R1} is the longest Rouse relaxation time, τ_R . The last term is a low-frequency portion of the relaxation mode representing the glassy nature, the G-mode defined in another series of study, associated with very short relaxation times.²¹

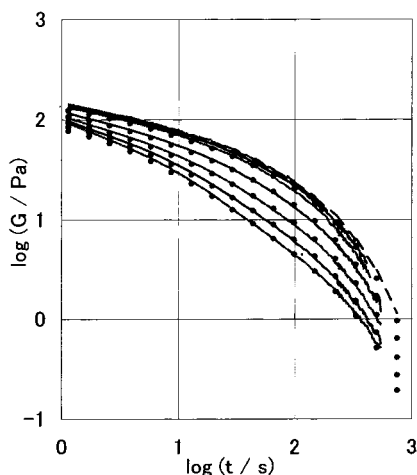


Figure 2. Strain-dependent relaxation modulus, $G(t, \gamma)$, at 273 K. Thin lines represent experimental data: $\gamma = 0.3, 0.7, 1.0, 2.0, 3.0, 4.0$, and 5.0 from top. Dots represent fitting function, eqs 13 and 14, for $\gamma = 1.0, 2.0, 3.0, 4.0$, and 5.0 . Dashed line at the top: linear relaxation modulus calculated from the parameters for linear viscoelasticity, eq 7.

Equations below are definitions for some of the usual parameters: A_G , coefficient of storage modulus; η , viscosity; G_N , entanglement modulus; a , power law coefficient of G' .

$$G' = A_G \omega^2, \quad G'' = \eta \omega \quad (\text{at the limit of } \omega = 0) \quad (8)$$

$$G' = G_N \quad (\text{at the inflection point of the } \log \omega - \log G' \text{ curve}) \quad (9)$$

$$G' = a \omega^{1/2} \quad (\text{at frequencies where } G' \text{ can be approximated by the power law}) \quad (10)$$

We obtain from the figure $A_G = 1.62 \times 10^6 \text{ Pa s}^2$, $\eta = 9.1 \times 10^3 \text{ Pa s}$, $G_N = 210 \text{ Pa}$, and $\log a = 1.55$. The relaxation time in slow steady flow, τ_w , which is essentially the longest stress relaxation time is

$$\tau_w = \frac{A_G}{\eta} = 180 \text{ s} \quad (11)$$

The entanglement molecular weight, M_e , is

$$M_e = \frac{cRT}{G_N} = 530 \text{ kg mol}^{-1} \quad (12)$$

and the number of entanglement per chain is $M/M_e = 10.3$. The longest Rouse relaxation time evaluated from the a value (eq 27) is 2.48 s in good agreement with the one, τ_{R1} , obtained in the process of curve fitting.

Strain-Dependent Relaxation Modulus. The strain-dependent relaxation modulus, $G(t, \gamma)$, is represented by a solid line in Figure 2. Measurements were performed at 298 K and reduced to 273 K with the method of reduced variables. The dashed line represents the relaxation modulus evaluated from the fitting parameters shown in eq 7. The data at $\gamma = 0.3$ is in good agreement with the curve except at short times, where the data may be too high, by less than 5%. The data at still shorter times, corresponding to less than 0.1 s of the raw data before reducing to the reference temperature, were discarded. For use of the data by other researchers, a fitting function was determined as

$$G(t, \gamma) = \sum_{p=1}^N g_p h_p(\gamma) \exp\left(-\frac{t}{\tau_p}\right) + \frac{cRT}{M} \sum_{p=1}^{N_R} g_{Rp} \exp\left(-\frac{t}{\tau_{Rp}}\right) \quad (13)$$

Here the mode-dependent damping function is given by

$$h_p(\gamma) = \frac{1}{1 + 0.2\gamma^2 \exp[-0.007(p-1)^3]} \quad (14)$$

Calculated values are represented by dots in Figure 2. No physical meaning was sought for the fitting function.

The relaxation modulus decreases with increasing magnitude of shear. The relative degree of decrease is larger at longer times. According to the presumption that $G(t, \gamma)$ is factorable as eq 1, we shifted the curves of Figure 2 vertically so that shifted curves superimpose with one another at long times: $G(t, \gamma)/h(\gamma)$ are plotted against time where $\log h(\gamma)$ represents the amount of shift for finite values of γ (Figure 3). The data at 100–200 s superimposed very well to form a single composite curve. The data at longer times are accompanied with more scattering but seem to be superimposed with use of the same values of $h(\gamma)$. In terms of the notation used in previous studies,⁵ the critical time, t_k , is about 100 s.

The damping function determined in this way can be fitted by

$$h(\gamma) = \frac{1}{1 + 0.2\gamma^2} \quad (15)$$

This is close to, but slightly higher than, the theoretical prediction of the Doi–Edwards tube model theory with independent alignment assumption.^{1–3a} A time-dependent damping function was defined as

$$h(t, \gamma) = \frac{G(t, \gamma)}{G(t, 0)} \quad (16)$$

and shown in Figure 3. Details of the variation of $h(t, \gamma)$ will be discussed later.

Shear Flow of Fixed Rate. The stresses in the start-up flow of constant rate are shown as functions $\eta(t, \dot{\gamma})$ and $\Psi_1(t, \dot{\gamma})$ in Figure 4. At low rates of shear, these quantities are increasing functions of time. The lowest rate of shear, 0.00065 s^{-1} , is much lower than $1/\tau_w$ and the corresponding data of η are in good agreement with those at the limit of $\dot{\gamma} \rightarrow 0$ (dashed curve). Ψ_1 was not obtained at such a low rate of shear. The curves at high rates of shear exhibit overshoot. Details of the variation are discussed soon. At the highest rate of shear, 4.9 s^{-1} , the flow was stable and the data were reproducible until about 200 s and then the stress began to change irregularly. At still higher rates of shear, the instability started at shorter times.

Steady values of η and Ψ_1 are shown in the upper panel of Figure 5, and time corresponding to the maximum of η or Ψ_1 in the transient state, t_m , is shown in the lower panel. Filled circles are for η and unfilled circles for Ψ_1 . The range of $\dot{\gamma}$ for t_m data represents the range where maximum of stress is detectable (at low $\dot{\gamma}$) and the peak position was the same in repeated experiments (at high $\dot{\gamma}$). The qualitative features of variation of various quantities in Figure 5 are well-known.^{3,21}

Discussion

Details of the Damping Function. In view of the construction procedure of upper panel of Figure 3, we

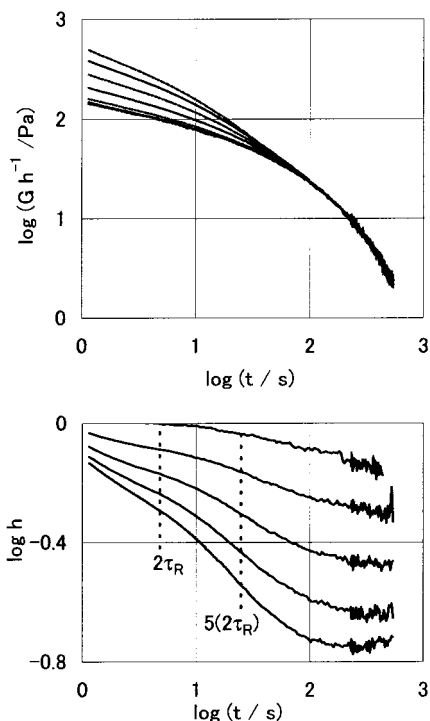


Figure 3. Upper panel: shifted relaxation modulus, $G(t, \gamma)/h(\gamma)$, at 273 K; $\gamma = 0.3, 0.7, 1.0, 2.0, 3.0, 4.0$, and 5.0 from bottom. Lower panel: time-dependent damping function, $h(t, \gamma)$; $\gamma = 1.0, 2.0, 3.0, 4.0$, and 5.0 from top.

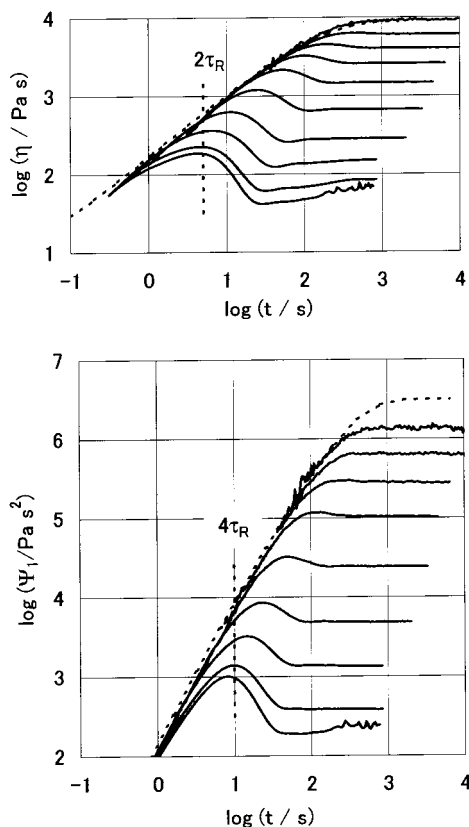


Figure 4. Viscosity growth function, $\eta(t, \gamma)$, (upper panel) and growth function of normal stress coefficient, $\Psi_1(t, \gamma)$, (lower panel) at 273 K. $\dot{\gamma}/s^{-1} = 0.00065$ (only for η), $0.0049, 0.0113, 0.0227, 0.049, 0.129, 0.392, 0.97, 2.59$, and 4.9 from top. Dashed lines represent values at the limit of $\dot{\gamma} \rightarrow 0$.

believe that each curve in lower panel levels off at about 100 s and the apparent decrease of $h(t, \gamma)$ at longer times

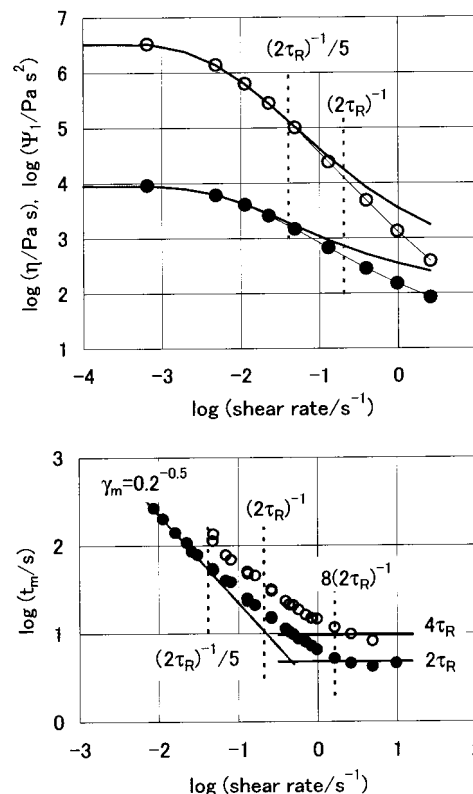


Figure 5. Upper panel: η (unfilled circles and thin line) and Ψ_1 (filled line and thin line) in steady shear flow. Thick lines represent K-BKZ calculation. Lower panel: Times corresponding to peaks of $\eta(t, \dot{\gamma})$ (filled circles) and $\Psi_1(t, \dot{\gamma})$ (unfilled circles).

is due to scattering of data. Using the earlier notation for the time of leveling off,⁵ we obtain

$$t_k = 100s = 21(2\tau_R) \quad (17)$$

The ratio $t_k/2\tau_R$ in previous reports was about 5, and t_k was claimed to be an explicit expression of a time sufficiently longer than $2\tau_R$.^{6,7} The present value is about 4 times larger. We believe that the difference comes from the different evaluation method, or definition, of τ_R in earlier studies. The present value of $t_k/2\tau_R$ is probably too large to regard t_k as a measure of sufficiently long time compared with $2\tau_R$.

An easy compromise may be to employ other definitions of τ_R , which usually give higher values. However, we stick to the starting policy of the study and examine the damping function in terms of the τ_R evaluated from $G^*(\omega)$.

A simple model of chain contraction by Doi^{8,22} gives

$$h(t, \gamma) = h(\gamma) \left[1 + \left(\sqrt{\frac{1}{h(\gamma)}} - 1 \right) f(t) \right]^2 \quad (18)$$

where f is a decreasing function of time representing the chain contraction process and is given in the paper. For simplicity, one may replace f by a function with one (the longest) relaxation time

$$f = \exp\left(\frac{-t}{2\tau_R}\right) \quad (19)$$

This function gives too rapid damping compared with the observed result. Original function by Doi, including shorter relaxation times, gives a still more rapid damp-

ing. The experimental data may be reproduced if a slower term is included, for example

$$f = \psi \exp\left(\frac{-t}{2\tau_R}\right) + (1 - \psi) \exp\left(\frac{-t}{2n\tau_R}\right) \quad (20)$$

Experimental results for $\gamma = 4$ and 5 are well approximated by choosing $\psi = 0.8$ and $n = 7$, and that for $\gamma = 1$, by choosing $\psi = 0$ and $n = 7$. Thus one possibility is that t_k is not necessarily related to the chain contraction process. The damping process for large strain may be dominated by the term with the contraction characteristic time, $2\tau_R$, although the term with longer relaxation time is not negligible. The term with longer time becomes more important at smaller strains.

The slow process is not included in the original tube model theory^{1,2} or its modifications.^{8–10} A characteristic feature of the process is that it is dominant for finite but small strains. A slow process is suggested in a paper by Mhetar and Archer but it may be concerned with highly entangled systems and at high strains.^{23,24} It may be due to a completely unknown type of molecular motion. On the other hand, detailed studies of the effect of finite strains on nonreptational relaxation mechanisms such as the constraint release²⁵ may also be necessary.

Features at Low Rates of Shear. As mentioned in the Introduction section, flow behavior at low $\dot{\gamma}$ hardly shows signs of characteristic time or rate related to the chain contraction. Overshoot of the first normal stress difference may be caused by the extension of chain contour length in excess of the equilibrium value. As seen in the lower panel of Figure 5, the overshoot of $\Psi_1(t, \dot{\gamma})$ was first detected at approximately

$$\dot{\gamma} = \frac{(2\tau_R)^{-1}}{5} \quad (21)$$

This is a reasonable value as the criterion for the rate sufficiently lower than $(2\tau_R)^{-1}$. So we examine other quantities around this rate of shear.

The K-BKZ model consistent with the tube model with independent alignment assumption gives the strain corresponding to the peak of $\eta(t, \dot{\gamma})$. For the damping function of eq 15, one obtains

$$\gamma_m = \dot{\gamma} t_m = 0.2^{-1/2} \quad (22)$$

This is represented by the slant line in the lower panel of Figure 5. The data points are on the line at low $\dot{\gamma}$ and deviate at $\dot{\gamma}$ higher than the value of eq 21. The K-BKZ model calculation was also done for the steady values and is shown in the upper panel of Figure 5 (thick lines). Again deviation of data points from the K-BKZ lines becomes detectable at the rate of eq 21. As seen in the figure, the deviation is the result of the concave shape of theoretical curves at high $\dot{\gamma}$, which in turn is due to the sharp decrease of $h(t, \dot{\gamma})$ at $t \approx 2\tau_R$. These deviations between the data and the K-BKZ calculation imply that the basic assumption of the original tube model, that the contour length is always constant, is not applicable at $\dot{\gamma}$ higher than that of eq 21. We may take eq 21 as the measure of sufficiently low $\dot{\gamma}$ for the contour length to remain at its equilibrium value.

Stress Overshoot at High Rates of Shear. The peaks of $\eta(t, \dot{\gamma})$ and $\Psi_1(t, \dot{\gamma})$ approximately correspond to

constant times, $2\tau_R$ and $4\tau_R$ (eqs 2 and 3), respectively, at high rates of shear

$$\dot{\gamma} > 8(2\tau_R)^{-1} \quad (23)$$

This observation is in accord with the modified tube model theory by Pearson et al.⁹ The intermediate range of rate of shear around $\dot{\gamma} = (2\tau_R)^{-1}$ may be regarded as the crossover range between the ranges of eqs 21 and 23. The position of the peaks of $\eta(t, \dot{\gamma})$ and $\Psi_1(t, \dot{\gamma})$ is reasonably understood with the assumption that the $2\tau_R$ value determined from the dynamic modulus is the characteristic time for contraction of chain contour length.

What If τ_R Is Longer? Other methods for determining τ_R give values much higher than the present one, for moderately entangled systems. The factor depends on the method and the value of entanglement molecular weight, M_e as discussed later. Let us see how our results change if the Rouse time is 4 times higher than the present value; $\tau_R' = 10$ s.

The time for leveling off of $h(t, \dot{\gamma})$ satisfies a relation, $t_k/2\tau_R' = 5$, which is in accord with earlier idea that t_k represents a *sufficiently longer time* for completion of chain contraction.^{6,7} On the other hand, the discussion around eq 20 would lead us to a result that the main contraction process is not the mode with characteristic time $2\tau_R'$ but one with a shorter time, corresponding to the second or third longest Rouse time. As for the low $\dot{\gamma}$ limit mentioned with respect to Figure 5, eq 21 is replaced by $\dot{\gamma} = (2\tau_R')^{-1}$, which means that the deviation from the low $\dot{\gamma}$ behavior is first detected exactly at the characteristic contraction rate, rather than at a rate sufficiently lower than that. The time corresponding to the peak of $\eta(t, \dot{\gamma})$ at high $\dot{\gamma}$ will be $t_{om} = \tau_R'/2$, in the place of $t_{om} = 2\tau_R$.

The present authors prefer the view through τ_R rather than τ_R' , mostly for aesthetic reasons. Some of the observations, e.g., one about t_{om} , may call for a renewal of modified tube theories if τ_R' is taken as the longest Rouse relaxation time.

Comments on Evaluation Methods of τ_R . At least three types of method for estimating τ_R , or definitions of τ_R in effect, have been proposed. Here we compare the τ_R value taken in this paper with those from other methods.

(A) This assumes that the viscosity, η , at a certain critical molecular weight, $M_c(\phi)$, is equal to one derived from the Rouse theory and that η is proportional to M^α at higher M , where ϕ is polymer volume fraction and α is typically 3.4–3.6.^{16,20}

$$\tau_{RA} = \frac{6M\eta}{\pi^2 cRT} \left(\frac{M_c}{M}\right)^{\alpha-1} \quad (24)$$

Widely cited values of parameters for polystyrene solutions are

$$M_c = 33\phi^{-1.3} \text{ kg mol}^{-1} \quad \text{and} \quad \alpha = 3.5 \quad (25)$$

(B1) To follow the tube model theory for determination of τ_R from the reptation time, τ_{rep} ,^{1,2} and approximate the latter with the longest stress relaxation time, τ_w , one uses

$$\tau_{RB1} = \frac{\tau_{rep}}{6N} = \frac{\tau_w}{6N} \quad (26)$$

where $N = M/M_e$ is the number of entanglement per molecule.

(B2) To follow the assumption included in modified tube model theories that τ_w at a certain critical molecular weight is related to the Rouse relaxation time, one uses^{9,10,26}

$$\tau_{RB2} = \frac{\tau_w}{4} \left(\frac{M_c}{M} \right)^{1.4} \quad (27)$$

(C) This fits the Rouse equation (second term on rhs of eq 6) to $G'(\omega)$ data at high frequencies where $G' = a\omega^{1/2}$.¹² The definition can be applied to any semidilute solutions, entangled or nonentangled. The following equation is a good approximation

$$\tau_{RC} = \left(\frac{aM}{1.111cRT} \right)^2 \quad (28)$$

It was shown in a previous paper that approximately the same value (τ_{RC}') is obtained with eq 24 if we take

$$M_c = 1.5M_e = 11\phi^{-1.4} \text{ kg mol}^{-1} \text{ (for } \phi < 0.1 \text{) and } \alpha = 3.4 \quad (29)$$

in the place of eq 25.¹²

The values for the present data are $\tau_{RA} = 14$ s, $\tau_{RB1} = 2.9$ s, and $\tau_{RC} = 2.4$ s (or 2.48 s with eq 28); $\tau_{RC}' = 2.3$ s; $\tau_{RB2} = 4.5$ s (assuming $M_c = 2M_e$ and $N = 10.3$), 2.6 s (assuming $M_c = 35/\phi \text{ kg mol}^{-1}$), and 8.5 s (assuming eq 25: $M_c = 33\phi^{-1.3} \text{ kg mol}^{-1}$).

It may be pointed out that τ_{RB1} is proportional to $M^{0.5}$ for moderately entangled systems. Nonreptational modes of motion²⁵ must be taken into account to get rid of the superfluous M dependence. Since τ_{rep} is higher than τ_w , the corrected value of τ_{RB1} will be higher than that from eq 26 and closer to τ_{RA} . In ref 26, the relation $M_c = 35/\phi \text{ kg mol}^{-1}$, believed to be applicable only at higher c , was chosen and low τ_{RB2} value close to τ_{RC} was used at moderate c because it gave good fit to steady shear data. So the τ_{RB2} of ref 26 was actually determined from *nonlinear viscoelasticity*. The author did not care much about its relation to linear viscoelasticity, but the present result indicates that τ_{RB2} of ref 26 is close to τ_{RC} .

Methods A and C are based on the observation that linear viscoelasticity of nonentangled systems is approximately described with equation of the Rouse theory.²⁷ Method C puts focus on the shape of relaxation spectrum over a certain time range while method A on the modes with long relaxation times. According to these two methods, τ_R/M^2 is a function of concentration and common to entangled and nonentangled systems. On the other hand, methods B1 and B2 start from the tube model theory and its relation to linear viscoelasticity behavior is represented by eqs 26 and 27, respectively. The τ_{RB} value may not necessarily be related to Rouse-like behavior of nonentangled systems. The present authors cannot find any a priori reason to choose one from these three methods.

Conclusion

We tried to find any sign of the change of chain contour in nonlinear viscoelasticity of an entangled

polymer system. The longest Rouse relaxation time, τ_R , evaluated from dynamic modulus at high frequencies was considerably lower than those from other preceding methods. However, the value $2\tau_R$ seemed to be a reasonable candidate of the contour length equilibration time. Features of stress in shear flow of constant rate indicated that $5(2\tau_R)$ was a measure of sufficiently long time and $(2\tau_R)^{-1/5}$ of a sufficiently low rate of shear for the contour length to be in equilibrium. The same was almost true for the strain-dependent relaxation modulus at large strains. However, an additional damping process with longer characteristic time was not negligible. This process was dominant at finite but small strains.

Acknowledgment. We thank Professor G. Marrucci for fruitful discussions.

References and Notes

- (1) Doi, M.; Edwards, S. F. *J. Chem. Soc., Faraday Trans. 2* **1978**, 74, 1802, 1818; **1979**, 75, 32.
- (2) Doi, M.; Edwards, S. F. *The Theory of Polymer Dynamics*; Clarendon Press: London, 1986; Chapter 7, p 218.
- (3) See for example, Larson, R. G. *Constitutive Equations for Polymer Melts and Solutions*; Butterworth: Boston, 1988; Chapter 3, p 79, and Chapter 4, p 119 (a); Chapter 1, p 4 (b); Chapter 2, p 60 (c).
- (4) Osaki, K.; Kurata, M. *Macromolecules* **1980**, 13, 671.
- (5) For a review, see: Osaki, K. *Rheologica Acta* **1993**, 32, 429.
- (6) Osaki, K.; Nishizawa, K.; Kurata, M. *Macromolecules* **1982**, 15, 1068.
- (7) Osaki, K.; Takatori, E.; Tsunashima, Y.; Kurata, M. *Macromolecules* **1987**, 20, 525.
- (8) Doi, M. *J. Polym. Sci. Polym., Phys. Ed.* **1980**, 18, 1005.
- (9) Pearson, D.; Herbolzheimer, E.; Grizzuti, N.; Marrucci, G. *J. Polym. Sci., Polym. Phys. Ed.* **1991**, 29, 1589.
- (10) Mead, D. W.; Larson, R. G.; Doi, M. *Macromolecules* **1998**, 31, 7895.
- (11) Osaki, K. *Kor.-Aust. Rheol. J.* **1999**, 11, 287.
- (12) Osaki, K.; Inoue, T.; Uematsu, T. *J. Polym. Sci., Polym. Phys. Ed.* **2001**, 39, 1704.
- (13) Archer, L. A. *J. Rheol.* **1999**, 43, 1555.
- (14) Key, A. Note No. 134; College of Aeronautics: Cranford: U.K., 1962.
- (15) Bernstein, B.; Kearsley, E. A.; Zapas, L. J. *Trans. Soc. Rheol.* **1963**, 7, 391.
- (16) Menezes, E. V.; Graessley, W. W. *J. Polym. Sci., Polym. Phys. Ed.* **1982**, 20, 1817.
- (17) Rouse, P. E. *J. Chem. Phys.* **1953**, 21, 1272.
- (18) Osaki, K.; Inoue, T.; Uematsu, T. *J. Polym. Sci., Polym. Phys. Ed.* **2000**, 38, 3271.
- (19) Ferry, J. D. *Viscoelastic Properties of Polymers*, 3rd ed.; Wiley: New York, 1980; Chapter 11.
- (20) See for example, Graessley, W. W. *Adv. Polym. Sci.* **1974**, 16, 1.
- (21) See for example, Inoue, T.; Osaki, K. *Macromolecules* **1996**, 29, 1595.
- (22) Osaki, K.; Watanabe, H.; Inoue, T. *Macromolecules* **1996**, 29, 3611.
- (23) Mhetar, V.; Archer, L. A. *J. Non-Newtonian Fluid Mech.* **1999**, 81, 71.
- (24) Islam, M. T.; Sanchez-Reyes, J.; Archer, L. A. *J. Rheol.* **2001**, 45, 61.
- (25) See for example, Watanabe, H. *Prog. Polym. Sci.* **1999**, 24, 1253.
- (26) Pattamaprom, C.; Larson, R. G. *Macromolecules* **2001**, 34, 5229.
- (27) Chapter 12 of ref 19.

MA011219G